Seabirds enhance coral reef productivity and functioning in the absence of invasive rats

Nicholas A J Graham[1,2], Shaun K Wilson[3,4], Pete Carr[5,6], Andrew S Hoey[2], Simon Jennings[7], M. Aaron MacNeil[2,8]

[1] Lancaster Environment Centre, Lancaster University, Lancaster, LA1 4YQ, UK

[2] ARC Centre of Excellence for Coral Reef Studies, James Cook University, Townsville, Queensland 4811, Australia

[3] Department of Biodiversity, Conservation and Attractions, Perth, Western Australia 6151, Australia

[4] Oceans Institute, University of Western Australia, Crawley, WA 6009, Australia

[5] Institute of Zoology, Zoological Society of London, London, NW1 4RY, UK

[6] College of Life and Environmental Sciences, University of Exeter, Exeter EX4 4QD, UK

[7] International Council for the Exploration of the Sea, H.C. Andersens Blvd 44-46, 1553 København V, Denmark

[8] Department of Biology, Dalhousie University, Halifax, NS, B3H 4R2, Canada

Biotic connectivity between ecosystems can provide major transport of organic matter and nutrients, influencing ecosystem structure and productivity[1], yet the implications are poorly understood due to human disruptions of natural flows[2]. When abundant, seabirds feeding in the open ocean transport large quantities of nutrients onto islands, enhancing the productivity of island fauna and flora[3,4]. Whether leaching of these nutrients back into the sea influences the productivity, structure, and functioning of adjacent coral reef ecosystems is not known. Here, we address this question using a rare natural experiment in the Chagos Archipelago, where some islands are rat-infested, while others are rat-free. We found that seabird densities and nitrogen deposition rates are 760 and 251 times higher on islands where humans have not introduced rats. Consequently, rat-free islands had substantially higher $\delta^{15}N$ values in soils and shrubs, reflecting pelagic nutrient sources. These higher values of $\delta^{15}N$ were also apparent in macroalgae, filter-feeding sponges, turf algae, and fish on adjacent coral reefs. Herbivorous damselfish on reefs adjacent to the rat-free islands grew faster, and fish communities had higher biomass across trophic feeding groups, with overall biomass 48% greater. Rates of two critical ecosystem functions, grazing and bioerosion, were 3.2 and 3.8 times higher adjacent to rat-free islands. Collectively, these results reveal how rat introductions disrupt nutrient flows among pelagic, island, and coral reef ecosystems. Rat eradication should be a high conservation priority on oceanic islands, likely to benefit terrestrial ecosystems and enhance coral reef productivity and functioning by restoring seabird derived nutrient subsidies from large areas of ocean.

The flow of organic matter and nutrients among ecosystems is a major determinant of productivity, composition, and functioning. Animals, such as moose[5], salmon[6], and sea turtles[7], can connect ecosystems by vectoring organic matter and nutrients between them. However, the magnitude and implications of these natural dynamics are poorly understood in contemporary ecosystems where humans have disrupted connectivity by creating barriers such as dams, removing biomass, and introducing predators[2,8]. Seabirds are globally important drivers of nutrient cycling[9], transferring nutrients from their pelagic feeding grounds to islands where they roost and breed[1,10]. This input of nutrient-rich guano increases plant biomass, alters plant species compositions, and enhances the abundance of many types of biota[3,4]. Nutrients can leach from guano to adjacent marine systems, which may bolster plankton densities and influence feeding behaviour of manta rays[11,12]. However, the effects of seabird transported nutrients on the productivity, structure, and functioning of highly diverse coral reefs is currently unknown. Understanding natural nutrient connectivity is particularly important, yet challenging, because invasive predators such as rats and foxes have decimated seabird populations within 90% of the world's temperate and tropical island groups[8].

Here, we isolate the effects of seabird-derived nutrients on adjacent coral reefs using a rare, large-scale natural experiment where some islands in a remote coral reef archipelago are rat-infested, while others are rat-free. The northern atolls of the Chagos Archipelago, central Indian Ocean, have been uninhabited by people for over 40 years, are protected from fishing, and host some of the world's most pristine marine environments[13]. Black rats (*Rattus rattus*) are thought to have been introduced to the archipelago in the late 1700s and early 1800s, but due to patterns of human habitation and movement, are not present on all islands. We use this unique scenario and a mixed-methods approach to investigate nutrient flux between oceanic, island, and coral reef ecosystems.

We studied six rat-free and six rat-infested islands, selected to be otherwise similar in terms of size, location and environment. Rats are known to predate upon bird eggs, chicks, and occasional adults, decimating populations where they have been introduced[8]. Mean seabird density, averaged across a 6-year period (Methods), was 760 times greater on rat-free than rat-infested islands (Fig 1a; 1243 birds/ha rat-free, 1.6 birds/ha rat-infested). These high seabird densities on some islands has led to Chagos having ten Important Bird and Biodiversity Areas[14]. Biomass of 14 bird species within six families varied among islands, with terns and noddy's contributing greatest biomass, and booby's, shearwaters, and frigate birds only common on some islands. Biomass of all species was greatest on rat-free islands (Fig. 1b).

We used species-specific abundance, body size scaled defecation rate, nitrogen content of guano[15], and mean residence times on the islands to estimate mean nitrogen input by the seabirds (Methods). Nitrogen input by seabirds per hectare of island was 251 times greater on rat-free islands than rat-infested islands (Fig 1c; 190 kg/ha/yr rat-free, 0.8 kg/ha/yr rat-infested). The nutrient input onto rat-free islands is comparable to nitrogen inputs by seabirds at the isolated and rat-free Palmyra atoll in the Pacific[15]. We did not calculate nutrient input from rats as they are recycling nutrients already present on the islands. In contrast, the majority of the seabirds feed in the open ocean, substantial distances from reefs (Extended Data Table 1). By foraging offshore, seabirds feed from food webs supported by net primary production that is estimated to be 2 to >5 orders of magnitude higher than net primary production on adjacent coral reefs (Methods; Extended Data Figure 1). Their capacity to access these oceanic prey resources leads to substantial deposition of oceanic nitrogen that would otherwise be unavailable on rat-free islands.

We used abundance of nitrogen and stable isotopes (reported as δ^{15}N) to understand uptake of nutrients on islands and in adjacent coral reef ecosystems (Methods; Fig. 2). Abundance and

δ^{15}N were strongly and positively correlated (r = 0.96), meaning that they show similar patterns in our samples. Soils on rat-free islands were enriched in ^{15}N, with δ^{15}N being 3.8 times higher than on rat-infested islands and comparable to reported values for seabird guano[16] (Fig. 2b). Substantially greater δ^{15}N was also evident in new growth leaves of a coastal plant (*Scaevola taccada*) on rat-free islands (Fig. 2c), indicating uptake of oceanic derived nutrients by island vegetation.

Nitrogen is expected to leach off islands to nearshore marine environments through rainfall and coastal advection[11]. On the reef flat (~1 m deep and 100 m from shore) filter feeding sponges (*Spheciospongia* sp; Fig 1d) and macroalgae (*Halimeda* sp; Fig 1e) had substantially higher δ^{15}N values near rat-free islands, though differences were smaller than observed for island soils and vegetation. This is consistent with findings of higher δ^{15}N values in corals closer to seabird colonies in New Caledonia[17]. On the reef crest (~3 m deep and 230 m (± 55 m StDev) from island shorelines) δ^{15}N was significantly higher in turf algae and herbivorous damselfish (*Plectroglyphidodon lacrymatus*) muscle adjacent to rat-free islands (Fig. 2f, g). While recognising the influence of trophic fractionation on δ^{15}N signatures, the relative depletion of the heavy isotope ^{15}N from soils across to the reef crest on rat-free islands, compared to the relatively stable values for rat-infested islands, provides strong evidence of seabird-vectored nutrient enrichment propagating out onto adjacent coral reefs. These diminishing effect sizes from the islands out to the reef crest likely reflect a range of processes, including uptake and conversion of nitrogen by micro- and macro-organisms across the reef flat[18].

Comparison of damselfish growth on reef crests (using growth bands in otoliths; Methods) demonstrated that individuals adjacent to rat-free islands were growing significantly faster towards their maximum expected size (K_r-K = -0.10 [-0.18, -0.04], net rat effect), and were larger for a given age than individuals on reefs adjacent to rat-infested islands (Fig. 3). This is

126 the first evidence for seabird-vectored nutrient subsidies propagating through the food web to
127 accelerate the growth of a marine vertebrate. Given the diversity and high biomass of fishes
128 that feed on benthic algae on coral reefs[19], this finding is likely to indicate higher fish
129 production adjacent to seabird dominated islands with repercussions for production of their
130 predators.

131 To assess the influence of seabird colonies on reef fish biomass production, we surveyed fish
132 communities along reef crests of the islands (Methods). Total biomass of the reef fish
133 community was 48% greater adjacent to rat-free islands. Assigning the 123 species of reef
134 fish recorded into feeding groups, we found biomass to be greater for all feeding groups of
135 fish on reefs adjacent to rat-free islands, with herbivore biomass having the largest effect size
136 (93% of posterior distribution above zero; Fig. 4a). These results are consistent with seabird-
137 vectored nutrients subsidising the entire ecosystem.

138 Herbivorous fish are functionally important on coral reefs, maintaining a healthy balance
139 between corals and algae, and clearing space for coral settlement[20]. Parrotfishes are among
140 the most abundant and important herbivorous groups, providing unique grazing and
141 bioerosion functions. We estimated grazing and bioerosion rates of parrotfishes for each
142 island using density data, along with species- and body size-specific information on
143 consumption rates[21] (Methods). Reef crests adjacent to rat-free islands are fully grazed 9
144 times a year, compared to 2.8 times for rat-infested islands (median values; Fig. 4b;
145 $Grazing_{rats}$-$Grazing_{no\ rats}$ = -1.18 [-2.24, -0.11], net rat effect). Although variable, median
146 bioerosion rates were 94 tonnes/ha/yr adjacent to rat-free islands, 3.8 times higher than the
147 24.5 tonnes/ha/yr adjacent to rat-infested islands (Fig. 4c; $Erosion_{rats}$-$Erosion_{no\ rats}$ = -1.06 [-
148 2.77, 0.53], net rat effect). Bioerosion is critical for breaking down dead substratum between
149 major disturbance events to provide stable substratum for new coral growth and recovery[20],
150 and for providing sand to maintain island growth in low lying atolls[22]. While some

151 bioeroding parrotfishes can take bites from corals, coral cover was not lower on rat-free
152 islands (coral cover rat-free = 26.3% ± 5.2 SE; rat-infested = 28.2 ± 5.5 SE). These data are
153 consistent with seabirds on rat-free islands enhancing key ecosystem functions on coral reefs.

154 Following our surveys, coral reefs of the Chagos Archipelago lost ~75% coral cover in the
155 2016 El Niño driven mass coral bleaching event[23]. It is possible that corals surrounding rat-
156 free islands will show greater resilience to this event than corals adjacent to rat-infested
157 islands, for two key reasons. Firstly, in contrast to nutrient inputs from anthropogenic
158 sources, nutrient delivery from biological sources such as fish and seabirds is rich in
159 phosphorus[3,24] which has been shown to enhance coral thermo-tolerance[25] and coral
160 calcification rates[24]. Secondly, greater grazing rates, as observed on reefs adjacent to rat-free
161 islands, is a key determinant of reef recovery[26].

162 Here, we have shown that seabird nutrient subsidies fuel the coral reef ecosystem, reflecting
163 natural productivity and functioning in the absence of introduced rats. Oceanic coral reefs,
164 such as those in the Chagos Archipelago, are highly productive ecosystems in an oligotrophic
165 environment, the mechanism of which has intrigued scientists for decades[27]. Seabird vectored
166 nutrient subsidies are clearly a major pathway through which this productivity is supported,
167 and such subsidies should be considered in the design and analyses of coral reef surveys
168 adjacent to oceanic islands.

169 Rat eradication has been successful on 580 islands worldwide, and although success rates are
170 slightly lower for tropical islands (89%) compared to temperate (96.5%), new techniques and
171 guidelines are expected to close this gap[28]. As eradication of rats from islands can lead to
172 immigration and positive growth rates of seabird populations[29], rat removal should be a
173 conservation priority for coral reef islands. The return of seabirds would benefit not only the
174 island ecosystem, but also adjacent nearshore marine ecosystems. In a time of unprecedented

threats to coral reefs from climate change[30], enhancing productivity and key ecosystem functions will give reefs the best possible chance to resist and recover from future disturbances.

1. Polis, G. A., Anderson, W. B. & Holt, R. D. Toward an integration of landscape and food web ecology: the dynamics of spatially subsidized food webs. *Ann Rev Ecol Syst* **28,** 289-316 (1997).
2. Doughty, C. E. *et al.* Global nutrient transport in a world of giants. *P Natl Acad Sci USA* **113,** 868-873 (2016).
3. Croll, D. A., Maron, J. L., Estes, J. A., Danner, E. M. & Byrd, G. V. Introduced predators transform subarctic islands from grassland to tundra. *Science* **307,** 1959-1961 (2005).
4. Fukami, T. *et al.* Above-and below-ground impacts of introduced predators in seabird-dominated island ecosystems. *Ecol Lett* **9,** 1299-1307 (2006).
5. Bump, J. K., Tischler, K. B., Schrank, A. J., Peterson, R. O. & Vucetich, J.A. Large herbivores and aquatic–terrestrial links in southern boreal forests. *J Anim Ecol* **78,** 338-345 (2009).
6. Hocking, M.D. & Reynolds, J.D. Impacts of salmon on riparian plant diversity. *Science* **331,** 1609-1612 (2011).
7. Bouchard, S.S. & Bjorndal, K.A. Sea turtles as biological transporters of nutrients and energy from marine to terrestrial ecosystems. *Ecology* **81,** 2305-2313 (2000).
8. Jones, H. P. *et al.* Severity of the effects of invasive rats on seabirds: a global review. *Conserv Biol* **22,** 16-26 (2008).
9. Otero, X. L., Peña-Lastra, S. De La., Pérez-Alberti, A., Ferreira, T. O. & Huerta-Diaz, M. A. Seabird colonies as important global drivers in the nitrogen and phosphorus cycles. *Nat Commun* **9,** 246 (2018).
10. Polis, G. A., & Hurd, S. D. Linking marine and terrestrial food webs: allocthonous input from the ocean supports high secondary productivity on small islands and coastal land communities. *Am Nat* **147,** 396–423 (1996).
11. McCauley, D. J. *et al.* From wing to wing: the persistence of long ecological interaction chains in less-disturbed ecosystems. *Sci Rep* **2,** 409 (2012).
12. Shatova, O., Wing, S. R., Gault-Ringold, M., Wing, L. & Hoffmann, L. J. Seabird guano enhances phytoplankton production in the Southern Ocean. *J Exp Mar Biol Ecol* **483,** 74-87 (2016).
13. MacNeil, M. A. *et al.* Recovery potential of the world's coral reef fishes. *Nature* **520,** 341-344 (2015).
14. Carr, P. in *Important Bird Areas in the United Kingdom Overseas Territories* (ed. Sanders S. M.) British Indian Ocean Territory. 37-55 (Royal Society for the Protection of Birds, 2006).
15. Young, H. S., McCauley, D. J., Dunbar, R. B. & Dirzo, R. Plants cause ecosystem nutrient depletion via the interruption of bird-derived spatial subsidies. *P Natl Acad Sci USA* **107,** 2072-2077 (2010).

16. Szpak, P., Longstaffe, F. J., Millaire, J-F. & White, C. D. Stable isotope biogeochemistry of seabird guano fertilization: results from growth chamber studies with maize (Zea mays). *PLOS ONE* **7,** e33741 (2012).
17. Lorrain, A. *et al.* Seabirds supply nitrogen to reef-building corals on remote Pacific islets. *Sci Rep* **7,** 3721 (2017).
18. MaMahon, K. W., Johnson, B. J., Ambrose, W. G. Ocean Ecogeochemistry: a review. *Oceanogr Mar Biol Ann Rev* **51,** 327-374 (2013).
19. Mora, C. Ecology of fishes on coral reefs. Cambridge University Press, Cambridge (2015).
20. Bellwood, D. R. *et al.* Confronting the coral reef crisis. *Nature* **429,** 827-833 (2004).
21. Hoey, A. S. & Bellwood, D. R. Cross-shelf variation in the role of parrotfishes on the Great Barrier Reef. *Coral Reefs* **27,** 37-47 (2008).
22. Perry, C. T., Kench, P. S., O'Leary, M. J., Morgan, K. M. & Januchowski-Hartley, F. Linking reef ecology to island building: Parrotfish identified as major producers of island-building sediment in the Maldives. *Geology* **43,** 503-506 (2015).
23. Sheppard, C. R. C. *et al.* Coral bleaching and mortality in the Chagos Archipelago. *Atoll Res Bull* **613,** 1-26 (2017).
24. Shantz, A.A. & Burkepile, D.E. Context-dependent effects of nutrient loading on the coral–algal mutualism. *Ecology* **95,** 1995-2005 (2014).
25. D'Angelo, C. & Wiedenmann, J. Impacts of nutrient enrichment on coral reefs: new perspectives and implications for coastal management and reef survival. *Curr Opin Environ Sust* **7,** 82-93 (2014).
26. Graham, N. A. J., Jennings, S., MacNeil, M. A., Mouillot, D. & Wilson, S. K. Predicting climate-driven regime shifts versus rebound potential in coral reefs. *Nature* **518,** 94–97 (2015).
27. Gove, J. M. *et al.* Near-island biological hotspots in barren ocean basins. *Nature Comms* **7,** 10581 (2016).
28. Keitt, B. *et al.* Best practice guidelines for rat eradication on tropical islands. *Biol Conserv* **185,** 17-26 (2015).
29. Brooke, M. de L. *et al.* Seabird population changes following mammal eradications on islands. *Anim Conserv* **21,** 3-12 (2018).
30. Hughes, T. P. *et al.* Spatial and temporal patterns of mass bleaching of corals in the Anthropocene. *Science* **359,** 80-83 (2018).

Acknowledgments This research was supported by the Australian Research Council's Centre of Excellence Program (CE140100020), a Royal Society University Research Fellowship awarded to N Graham (UF140691), and a Tier II NSERC Research Chair awarded to A MacNeil. We thank the British Indian Ocean Territory section of the British Foreign and Commonwealth Office for permission to conduct the study, and Dr John Turner for organising the expedition. Animal ethics for fish collection was approved by James Cook University (approval number A2166). Many thanks to J. Lokrantz for graphics help with figures 1 and 2, and J. Barlow, S. Keith, and R. Evans for comments on the manuscript.

Author Contributions N.A.J.G. conceived of the study with S.K.W.; N.A.J.G., S.K.W., and P.C. collected the data; N.A.J.G., M.A.M, S.J., and A.S.H. developed and implemented the analyses; N.A.J.G. led the manuscript with S.K.W., M.A.M., S.J., A.S.H., and P.C.

Author Information

Reprints and permissions information is available at www.nature.com/reprints. The authors declare no competing financial or non-financial interests. Correspondence and request for materials should be addressed to N.A.J.G. (nick.graham@lancaster.ac.uk)

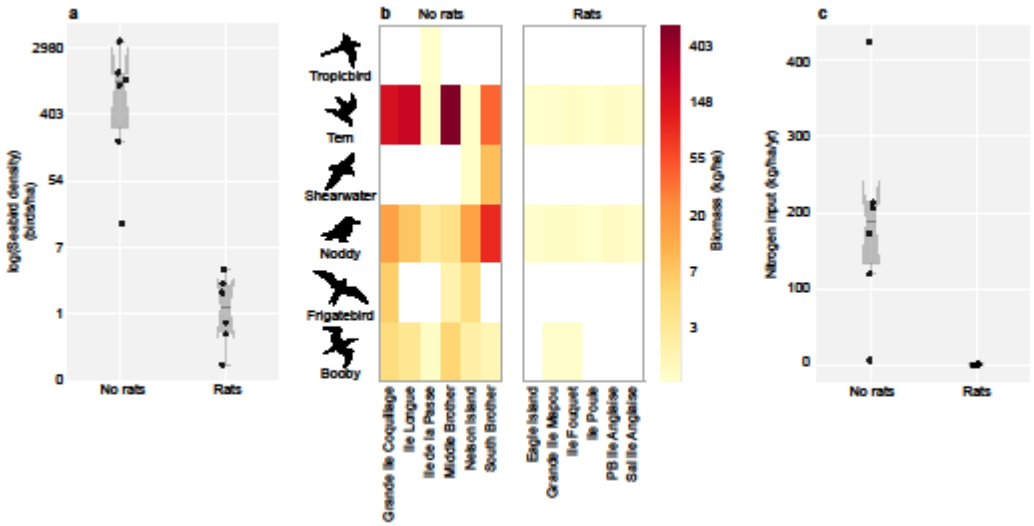

Figure 1 | Seabird densities, biomass, and nitrogen input to islands with and without rats in the Chagos Archipelago. a) Seabird density on rat-free (n = 6) and rat-infested (n = 6) islands. b) Heatmaps of seabird biomass per family, on each island. Tropicbird: *Phaethon lepturus*; Tern: *Thallasseus bergii*, *Sterna sumatrana*, *Sterna dougallii*, *Onychoprion fuscatus*, *Onychoprion anaethetus*, *Gygis alba*; Shearwater: *Puffinus bailloni nicolae*, *Ardenna pacifica*; Noddy: *Anous tenuirostris*, *Anous stolidus*; Frigatebird: *Fregata sp.*; Booby: *Sula sula*, *Sula leucogaster*. c) Nitrogen input by seabirds per hectare for rat-free (n = 6) and rat-infested (n = 6) islands. Panels a) and c) are notched box plots, where the horizontal line is the median, box height depicts the interquartile range, whiskers represent 95% quantiles, and diagonal notches illustrate approximate 95% confidence intervals around the median. Estimated net rat effects (median [95% highest posterior density intervals]) are a) 456 [22, 6393] birds/ha; b) 195 [184, 207] kg/ha (total biomass); and c) 148 [81, 211] kg/ha/yr.

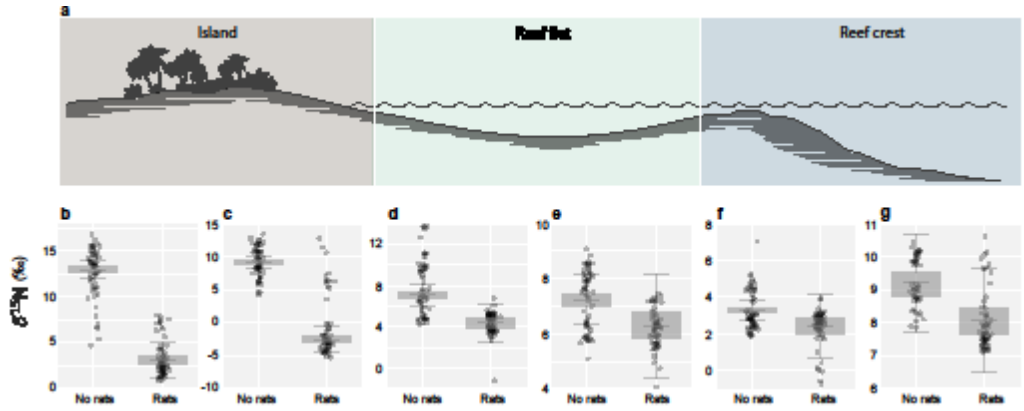

Figure 2 | Nitrogen isotope signals from islands to reefs in the presence and absence of invasive rats. a) Schematic of study system. δ^{15}N values for b) soil, and c) new growth leaves (*Scaevola taccada*) on islands, d) filter feeding sponges (*Spheciospongia* sp), and e) macroalgae (*Halimeda sp.*) on reef flats, and f) turf algae, and g) dorsal muscle tissue of damselfish (*Plectroglyphidodon lacrymatus*) on reef crests. For all samples, n = 120 were collected, except for panel g), where n = 110 (Methods). Panels b-g are box plots, where the horizontal line is the median, box height depicts first and third quartiles and whiskers represent the 95th percentile. Net rat effect (median [95% highest posterior density] and P(neg), the probability of effect being less than zero) estimates are b) soil -9.9 [-11.3, -8.4] P(neg)>0.99; c) leaves -11.8 [-13.2, -10.2] P(neg)>0.99; d) sponge -1.0 [-2.3, 0.5] , P(neg)=0.92; e) macroalgae -2.7 [-4.1, -1.23] P(neg)>0.99; f) turf -0.8 [-2.23, 0.6] P(neg)=0.90; g) fish -1.1 [-2.5, 0.3] P(neg)=0.94.

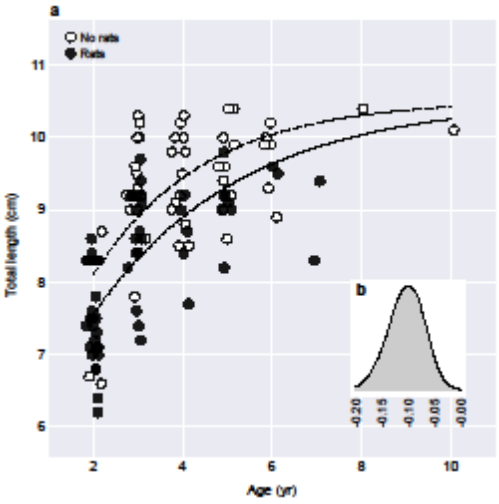

Figure 3 | Growth of herbivorous damselfish on coral reefs adjacent to islands with and without rats. a) Age by length growth curves for *Plectroglyphidodon lacrymatus* on rat-free (open circles) and rat-infested (closed circles) islands. b) Effect size posterior density for the difference between the growth parameter, *K* (yr^{-1}), on rat-free compared to rat-infested islands. n = 48 rat-free, and n = 58 rat-infested biologically independent samples.

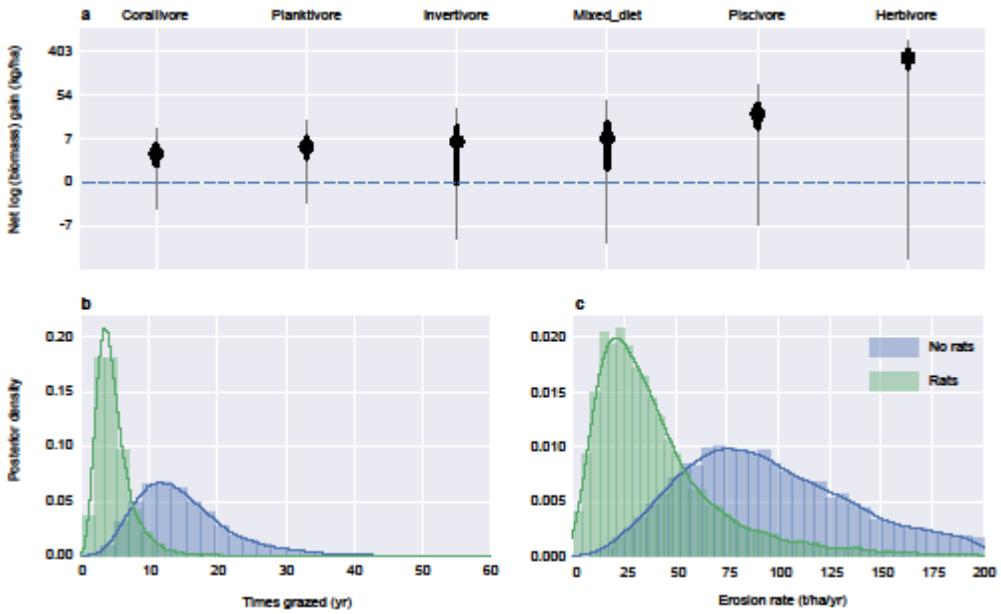

Figure 4 | Biomass and functioning of reef fish communities adjacent to islands with and without rats. a) Effect size plots from a hierarchical Bayesian analysis of fish biomass for different feeding groups between rat-free and rat-infested islands. n = 24 rat-free, and n = 24 rat-infested biologically independent surveys. Circles represent means, and dark and grey bars represent 50% and 95% uncertainty intervals, respectively (highest posterior density). Positive values correspond to greater biomass on rat-free islands. b) Effect size posterior density distributions for the proportion of reef grazed by parrotfishes each year on islands that are rat-free versus rat-infested. c) Effect size posterior density distributions for the volume of reef carbonate removed by parrotfishes each year on rat-free versus rat-infested islands.

METHODS

Study sites. The Chagos Archipelago (British Indian Ocean Territory) is situated in the central Indian Ocean, due south of the Maldives (5º 50' S, 72º 00' E). The archipelago was first discovered in the early 1500s, but was not settled until the 1700s, after which rats were inadvertently introduced to some islands of the territory[31]. In the early 1970s the British government established a lease of the southernmost atoll (Diego Garcia) to the US Navy for a military base, and resettled the Chagossian people in Mauritius, Seychelles, and the UK. Since that time, the atolls of the northern archipelago have had very few direct human impacts[32], with exceptionally high reef fish biomass[33], very low levels of water pollution[34], and there are currently 10 designated (2 more proposed) Important Bird and Biodiversity Areas[14]. However, invasive rats remain on a number of islands, creating a natural experiment to study the influence of rats on relatively undisturbed oceanic islands. In March-April 2015, we conducted research at 12 islands of similar size, across three atolls (Extended Data Table 2). Six of the islands were chosen as they are rat-free, while the other six are rat-infested.

Seabird surveys. Breeding seabird densities on each island were counted annually by P.C. from 2009-2015 using the apparently occupied nests methodology (AONs)[35,36]. The entire coastline of each island was surveyed first and AONs directly counted. Following the coastal survey, the interior of the island was searched. There were no breeding seabirds in the interior of Ile Poule, Grand Ile Mapou, Ile Fouquet, Eagle Island, and both Ile Anglaise islands. On islands where the interior search revealed breeding seabirds, techniques to estimate AONs varied by family. Brown Booby (*Sula leucogaster*) AONs were directly counted. Red-footed Booby (*Sula sula*) AONs were counted directly except on Nelson Island, and Grand Ile Coquillage. On these islands the total surface area of the breeding population was calculated

using a handheld Global Positioning System (GPS) and random plots of the area were counted for AONs. Plot size and whereabouts was directed by accessibility, visibility and the vulnerability of the breeding population. The means of the AONs of the plots were multiplied by the number of plots possible in the mapped area to estimate total AONs. Breeding frigatebirds (*Fregata sp.*) on Nelson Island and Grand Ile Coquillage were estimated using the same technique described above for Red-footed Booby. No tropicbird (*Phaethon lepturus*) nesting cavities were located, so tropicbird breeding numbers were estimated by counting aerial displaying pairs above islands or nest-prospecting adults in an appropriate habitat. Shearwaters (Procellariidae) nest in burrows, with the largest colony on South Brother island and some also on Nelson Island. Burrows is a loose term that covers rock fissures, crevices, tree roots, coconut boles, and various underground holes. Island surface area where burrows are present was estimated and AONs estimated by multiplying from an average burrow density, taken from random 10 m^2 sample plots throughout the island. Burrows were assumed occupied when a bird or egg was seen in them, there were indications of use (e.g. feathers, droppings), or they were heavily scented with shearwater musk. Burrows were assigned to either one of the shearwater species by identification of large chicks, eggs, or adults. For the arboreal breeding Noddy's (*Anous spp.*), direct counts were impractical for the large colonies on South Brother and Nelson Island, where subsampling and multiplication to the total colony area was used. All ground nesting tern species (Sternidae) with the exception of Sooty Tern (*Onychoprion fuscatus*) had AONs directly counted. To calculate the number of Sooty Tern AONs, the total colony area was mapped and random sample plots were counted for AONs to multiply up to the total area. Plot size was dictated by accessibility, visibility, and to avoid disturbing dense aggregations of breeding birds, with numbers counted from outside the colony at random points around the perimeter. While vegetation type, such as coconut versus native forests, can also affect bird densities[15], much

447 of the indigenous island vegetation has been lost in Chagos[14], and we used absolute bird
448 count estimates per island for this study.
449
450 Total annual seabird abundance was calculated based on the number of AONs multiplied by
451 the mean number of birds occupying those nests per species, and the period of the year that
452 the birds are present on the islands. For most species, a conservative 3 birds per nest was used
453 (2 adults and 1 chick), but some, for example sooty terns (*Onychoprion fuscatus*) have 1
454 adult, or 1 adult and 1 chick present for periods of the year, and others (e.g. red-footed booby
455 (*Sula sula*)) have a chick and 1-2 juvenile/immature birds present in the nest or sub-colony
456 area. Period of year spent on the island varied by species, from year round for species such as
457 the brown booby (*Sula leucogaster*) and common white tern (*Gygis alba*), to 4 months for the
458 roseate tern (*Sterna dougallii*). Biomass of bird species was estimated using the average mass
459 of an individual of each species taken from the Handbook of the Birds of the World[37].
460
461 We estimated the total nitrogen input from guano per hectare per year of each island
462 following Young et al. (15):
463
464
465 $$NI_{ij} = \frac{Ng \times Dr_i \times Bd_{ij} \times Res_{ij}}{IsArea_j}$$
466
467
468 where nitrogen input per hectare per year (*NI*) is estimated from the nitrogen content of
469 guano (*Ng*), the defecation rate in g per species of bird (*i*) per day (*Dr*), the number of that
470 species of bird (*Bd*) on the island (*j*), the number of days of the year that the species is
471 resident on the island (*Res*), and the area of the island (*IsArea*). Following (15), nitrogen
472 content of guano was held at 18.1% based on guano samples from similar species in the

473 Pacific. The contribution of guano (g) was based on the red-footed booby and scaled for other
474 species based on species biomass, assuming allometric relationships with body size[15]. We
475 adjusted the *Bd* estimates to account for time off islands during feeding forays. Given
476 uncertainties in foraging durations and whether birds would have full crops and bowels, it is
477 hard to be completely precise in these calculations. We assigned the 14 species into 3 groups,
478 which accounts for foraging excursions off island in a fairly conservative way. Group 1:
479 *Tropical shearwater, wedge-tailed shearwater, white-tailed tropicbird, sooty tern, brown*
480 *noddy, and frigatebirds*. Foraging will vary during the breeding cycle, but often one adult is
481 foraging and may be off the island overnight. We therefore assumed only one adult of the
482 pair was on the island at any one time. Group 2: *Red-footed booby*. One bird of the pair
483 makes daylight foraging forays but returns overnight. Adult numbers were therefore halved
484 only during daylight hours (12 hours). Group 3: *Great crested tern, roseate tern, black-naped*
485 *tern, common white tern, bridled tern, brown booby, lesser noddy*. In Chagos, these species
486 tend to make much shorter foraging forays (1-4 hours depending on species), meaning
487 defecation at sea will be minimal compared to land. We therefore did not make any
488 adjustments to their numbers.
489
490 Seabird densities per hectare of rat-free versus rat-infested islands were plotted as notched
491 box plots, where the horizontal line is the median, box height depicts the interquartile range,
492 and diagonal notches in the boxes illustrate the 95% confidence interval around the median[38].
493 The biomass of families of birds per island were plotted as log-scale heat maps for rat-free
494 and rat-infested islands. Nitrogen input for rat-free versus rat-infested islands were plotted as
495 notched box plots of kg per hectare per year. We also developed a set of simple Bayesian
496 models to estimate the net rat effects on log-scale bird numbers, log-scale total biomass, and
497 nitrogen input between rat-free and rat-infested islands:

$$y_i \sim N(\mu_i, \sigma_t)$$

$$\mu_i = \beta_0 + \beta_1 * RAT$$

$$\beta_x \sim N(0,10)$$

$$\sigma_t \sim U(0,10)$$

where y_i was the response variable, RAT was a dummy variable for rat-infested islands, and variances were estimated independently within treatments. The β_1 parameters being the rat effect sizes reported in the caption of Figure 1 along with the proportion of β_1 posterior density below zero.

Primary production and potential prey biomass and production available to seabirds. Biomass, production, and size-structure of consumers in the ocean surrounding the Chagos Islands were calculated from the primary production available to support them using a size-based model that characterises some of the main factors affecting the rate and efficiency of energy processing in marine ecosystems[39]. Briefly, these factors are (i) temperature, which affects rates of metabolism and hence growth and mortality; (ii) the size of phytoplankton and the predator to prey body mass ratio, which determine the number of steps in a food chain; and (iii) trophic transfer efficiency, a measure of energy conserved and lost at each step in the chain. In the model, size composition of the phytoplankton community is predicted from primary production and temperature using empirical relationships and, in turn, this size composition is used to estimate particle export ratios that influence transfer efficiency in the first steps of the food chain. The model is depth integrated and we made the simplifying assumption that all primary production occurs in the euphotic zone. We did not explicitly model production of benthic communities, but these would not be accessible to seabirds. In the model, relationships between primary consumer production and consumer production at any higher trophic level are determined by trophic transfer efficiency. Production at a

given body mass or trophic level was converted to biomass and numbers at the same body mass or trophic level based on the assumption that body size and temperature determined individual rates of production[39]. The modelled size-spectrum was discretised into units of 0.1 (log_{10}) for analysis.

The environmental data used to force the models comprised annual mean estimates of depth integrated primary production (g C m^{-2} d^{-1}) and sea surface temperature (°C) as derived from monthly predictions for the years 2010- 2012. Chlorophyll and primary production were obtained from the Mercator Ocean Project (Global Biogeochemical Analysis Product , BIOMER1V1 monthly 0.5° degree resolution)[40] and monthly temperature data from the Mercator Ocean physical NEMO model (PSY3V3R1)[41]. Inputs to the size-based models were allocated to a 0.5° grid that covered the sea area defined by the maximum foraging distance of the species of seabird, assumed to be a radius, such that foraging areas were circular around the islands (Extended Data Table 1). These distances are an approximation from the published literature, given foraging ranges can vary geographically[42]. Cells were assigned a mixed layer depth (m) and total depth (m)[43,44]. Mean biomass and production for organisms in body mass (wet weight) classes 0.1-9 g (smaller prey) and >1-50 g (larger prey) was estimated per unit area by grid cell, to approximate size ranges consumed by the seabird species based on prey size information in the literature and body mass class[45,46]. To address considerable uncertainty in model parameters, we ran 10000 simulations for each biomass or production estimate in each grid cell, with parameter estimates in each simulation drawn randomly from appropriate distributions. When parameters were correlated, the parameter estimates were drawn from multivariate distributions[39]. Model results were expressed as medians and percentiles calculated from the distribution of output values. Conversions from carbon to wet weight were based on published values[39,47]. Estimates of nitrogen content in

548 prey size classes were based on an assumed C:N ratio of 3.4:1, which is a typical value for
549 fish[48] and reflects the falling C:N ratio with trophic level in food webs that are supported by
550 primary producers with C:N ratios typically averaging 6.6:1 (ref. 49,50). Estimates of
551 biomass and production per unit area were converted to estimates of total biomass or
552 production in the foraging area of each bird species (Extended Data Table 1, Extended Data
553 Figure 1).
554
555 While rates of gross primary production can be high on coral reefs, net primary production,
556 although variable in space and time, is typically comparable with net primary production in
557 the more productive areas of the tropical ocean[51,52]. Given the area of reef surrounding the
558 rat-free islands is approximately 1.02 km^2, while foraging areas are >105 km^2 for 14 of the 15
559 bird species using these islands, large numbers of seabirds can feed from oceanic food webs
560 with much higher production that those on the reefs (Extended Data Figure 1). Even the
561 production estimates for prey in the size-ranges eaten by the seabirds are typically 3 or more
562 orders of magnitude higher than the expected primary production on this area of reef (0.0001
563 Tg C yr^{-1}, if mean on-reef primary production is assumed to be 0.3 g C m^{-2} d^{-1})[51]. Given the
564 numbers of seabirds and the extent of the prey resource they have the potential to access, the
565 strong signal from guano derived nitrogen on the reefs surrounding rat-free islands is
566 unsurprising. While the model has a number of assumptions, the results do highlight that
567 oceanic production in the foraging area is expected to be several orders of magnitude higher
568 than production on the reefs surrounding the islands and therefore that the higher levels of
569 connectivity that result from higher seabird abundance have the potential to transport
570 relatively high quantities of nitrogen to the reef systems.
571

572 **Isotope sampling.** From each island, 10 samples of topsoil (<5 cm from surface) were taken
573 from just behind the coastal vegetation boundary. Loose leaf litter and other vegetation was
574 cleared to expose the soil, and samples were taken a minimum of 10 m apart. Along the
575 beach margin of each island, new growth leaf samples were taken from 10 *Scaevola taccada*
576 plants. On the reef flat of each island, ~1 m deep and approximately 100 m from shore, 10
577 samples of filter feeding sponges (*Spheciospongia* sp.) and macroalgae (*Halimeda* sp.) were
578 taken from individual colonies and thalli, respectively. On the reef crest of each island, ~3 m
579 deep and 230 m (± 55m StDev) from shore, 10 turf algal samples were taken from dead
580 corals. Ten territorial herbivorous damselfish (*Plectroglyphidodon lacrymatus*) individuals
581 were collected by hand spear on the reef crest of each island in the same area the turf algae
582 were collected. Fish were euthanized on ice. Fish samples could not be collected from Nelson
583 Island. A sample of dorsal white muscle was taken from each fish. All samples were dried in
584 a drying oven at 60ºC for 24 hours or until fully dry. Samples were powdered with a pestle
585 and mortar and stored in sealed plastic sample vials.
586
587 Stable isotope analysis of nitrogen for all samples was carried out at the University of
588 Windsor, Canada. Isotope ratios were calculated from 400 to 600 μg of each sample added to
589 tin capsules and analysed with a continuous flow isotope ratio mass spectrometer (Finnigan
590 MAT Deltaplus, Thermo Finnigan, San Jose, CA, USA). Total nitrogen content (%) was also
591 estimated. Stable isotope values for nitrogen are expressed as delta (δ) values for the ratio of
592 ^{15}N:^{14}N. Turf, sponge, soil and macroalgae samples were acid washed with hydrochloric acid
593 to dissolve any calcareous matter or sediments that may have contaminated the samples.
594 Subsets of samples that were run with and without the acid wash had correlation coefficients
595 between 0.9 (turf) and 0.99 (soil), and all samples from rat-free and rat-infested islands were
596 treated the same. The standard reference material was atmospheric nitrogen. Samples were

run twice, with select samples run in triplicate to ensure accuracy of readings. Accuracy was within 0.3 ‰ for soil and within 0.1 ‰ for other samples, based on soil Elemental microanalysis B2153 and USGS 40 internal standards, respectively.

δ^{15}N values between rat-free and rat-infested island treatments were analysed using Bayesian hierarchical models, with area of reef surrounding each island (RA; calculated using GIS) as a covariate, and samples nested within their specific atoll. Distance to shore from the reef crest (DS) was used as an additional covariate for the turf algae and fish muscle samples. Models were run using the PyMC3 package[53] in Python (www.python.org), including a t-distribution with df=4 as:

$$\delta^{15}N_{oij} \sim t_4(\mu_{oij}, \sigma_0)$$

$$\mu_{oij} = \beta_{0i} + \beta_{1o} + \beta_{2o}RA + \beta_3 DS$$

$$\beta_{0i} \sim N(\gamma_0, \sigma_\gamma)$$

$$\beta_x, \gamma_0 \sim N(0, 1000)$$

$$\sigma_0, \sigma_\gamma \sim U(0, 100)$$

where each organism (o) had their own offset (β_1) relative to island-level (i) soil intercepts (β_0). Models were examined for convergence and fit by consideration of stability in posterior chains, Gelman-Rubin (R-hat) statistics, and the fit of the models with the data[54]. A gist of the PyMC3 code used for the δ^{15}N model is available at:
https://gist.github.com/mamacneil/42a426997b73b6283d3e50bc1c95a9a9

Fish growth. The total length of each damselfish (*Plectroglyphidodon lacrymatus*) sampled was carefully measured to the nearest mm. The paired sagittal otoliths (ear bones) were removed from each individual to estimate age[55]. One otolith from each pair was weighed to the nearest 0.0001 g and affixed to a glass slide using thermoplastic glue with the primordium located just inside the edge of the slide and the sulcul ridge perpendicular to the slide edge. The otolith was ground to the slide edge using a 600 grit diamond lapping disc on a grinding wheel along the longitudinal axis. The otolith was then removed and re-affixed to a clean slide with the flat surface against the slide face and ground to produce a thin transverse section c. 200 μm thick, encompassing the core material. Finally, the exposed section was covered in thermoplastic glue to improve clarity of microstructures. Sections were examined twice and age in years was estimated by counting annuli (alternating translucent and opaque bands) along a consistent axis on the ventral side of the sulcul ridge, using transmitted light on a stereo microscope.

Growth curves for the otoliths from the rat-free versus rat-infested islands were modelled using the three-parameter van Bertalanffy growth function, implemented in PyMC3 as:

$$\log(L_t) \sim N(\mu_i, \sigma_0)$$

$$\mu_i = \log(L_\infty - (L_\infty - L_0)e^{-(k_0+k1)t}))$$

$$k_0 \sim U(0.001, 1)$$

$$k_1 \sim N(0, 10)$$

$$L_0 \sim N(0, minL)$$

$$L_\infty \sim U(maxL, maxL \times 2)$$

$$\sigma_0 \sim U(0, 1000)$$

Where L_t is the observed total length (cm) at age t (years), L_∞ is the estimated asymptotic length, K is the coefficient used to describe the curvature of growth towards L_∞ (here split into k_0 (no rats) and k_1 (rat offset)) and L_0 is the theoretical length at age zero[56]. We specified uniform bounds for the L parameters based on observed minimum ($minL$=6.2) and maximum ($maxL$=10.4) fish lengths. Again, models were examined for convergence and fit by consideration of stability in posterior chains, R-hat statistics, and the fit of the models with the data. A gist of the PyMC3 code used for the von Bertalanffy model is available at: https://gist.github.com/mamacneil/6970e4ff88768532635dd44a682f7b9d

Fish biomass and function. Underwater visual surveys were conducted along the reef crest of each island. Four 30 m transects were laid along the reef crest at 3 m depth, separated by at least 10 m. Benthic cover of corals, algae, and other organisms were surveyed using the point intercept method, whereby the substratum type under the transect tape every 50 cm was recorded. The structural complexity of the reef was estimated visually on a 6 point scale, ranging from no relief to exceptionally complex (>1 m high) relief with numerous caves and overhangs. This structural complexity measure captures landscape complexity, including the complexity provided by live corals, that of the underlying reef matrix and other geological features, and has been shown to correlate well to other measures of complexity, such as measures of reef height and the linear versus contour chain method[57]. The density and individual sizes of diurnally active, non-cryptic species of reef-associated fish were estimated along each transect. Larger, more active fish were surveyed on the first pass of each transect in a 5 m wide belt, while the more territorial and abundant damselfish family (Pomacentridae) were surveyed on a second pass of the transect in a 2 m wide belt. We converted data on fish counts to biomass with published length–weight relationships[58,59]. Fish were assigned to feeding groups based on their dominant diets and feeding behaviour[60].

671

672 The grazing and erosion potential (i.e. area of reef scraped, and volume of carbonates
673 removed, respectively) by parrotfishes at each site was calculated as the product of feeding
674 rate, bite dimension (area or volume), and fish density (following[21]). Size-specific feeding
675 rates for each species were derived from best-fit regressions of bite rate (bites min^{-1}) and fish
676 length (total length, cm) for each species. Bite rates were quantified at three locations (Lizard
677 Island, northern Great Barrier Reef, northern Sumatra, Indonesia, and the central Red Sea)
678 using focal feeding observations. An individual parrotfish was haphazardly selected, followed
679 for a short period of acclimation (~1 min) during which the fish length (total length, TL) was
680 estimated to the nearest centimetre. Following the acclimation period each fish was followed
681 for a minimum of 3-minutes during which the number of bites on different benthic substrata
682 (primarily epilithic algal matrix and live corals) and observation time was recorded. Bite rates
683 were then converted to bites min^{-1}. Observations were discontinued if the focal individual
684 displayed a detectable response to the diver. All feeding observations were conducted during
685 0900-1500h with a minimum of 25 observations conducted per species per location.

686 The area (mm^2) and volume (mm^3) of material removed per bite by individual parrotfish was
687 estimated from species-specific relationships between bite size and fish length. To estimate
688 bite area an individual parrotfish was haphazardly selected, its total length estimated and
689 followed until it took a bite from the reef substratum. The dimensions of the bite (length and
690 width) were then measured in situ using dial callipers. A minimum of 16 observations (mean
691 = 34.3 observations) were made per species, with all observations performed at Lizard Island,
692 northern GBR. Bite volumes of species were largely taken from the literature[61], and
693 supplemented with in situ observations at Lizard Island for *Chlorurus microrhinos*. Where
694 possible species-specific bite rates and bite dimensions were used, when these were not
695 available, values for closely related congeners were used.

Total biomass and biomass of each trophic feeding group of fish (BIO_f) was modelled using Bayesian hierarchical models, with observations (j) nested within atolls (i) and including factors that could influence fish biomass as covariates; coral cover (HC), reef structural complexity (SC), and distance to shore (DS). The general model was:

$$\log(BIO_{fij}) \sim N(\mu_{fi}, \sigma_0)$$

$$\mu_{fi} = \beta_{f0i} + \beta_1 RAT + \beta_2 SC + \beta_3 HC + \beta_4 DS$$

$$\beta_{f0i} \sim N(\gamma_{f0}, \sigma_\gamma)$$

$$\beta_x, \gamma_{f0} \sim N(0, 1000)$$

$$\sigma_0, \sigma_\gamma \sim U(0, 100)$$

with models examined for convergence and fit by consideration of stability in posterior chains, R-hat statistics, and the fit of the models with the data. A gist of the PyMC3 code used for the fish biomass models is available at:
https://gist.github.com/mamacneil/b8025fe7805d2a86930eda056d60a9a8

The two ecosystem functions, grazing and erosion potential (rounded to nearest whole number), where modelled with the same Bayesian hierarchical structure, but with an alternative Poisson (Pois) rate (XR) likelihood:

$$XR_{ij} \sim Pois(e^{\mu_{ji}})$$

$$\mu_{ji} = \beta_{j0i} + \beta_1 RAT + \beta_2 SC + \beta_3 HC$$

$$\beta_{j0i} \sim N(\gamma_{j0}, \sigma_\gamma)$$

$$\beta_x, \gamma_{j0} \sim N(0, 1000)$$

$$\sigma_0, \sigma_\gamma \sim U(0, 100)$$

A gist of the PyMC3 code used for the grazing model is available at:

https://gist.github.com/mamacneil/884836392f4b09efc7f7daf67a73e02f

A gist of the PyMC3 code used for the erosion model is available at:

https://gist.github.com/mamacneil/3cbea63ad422e55120a0744acc836ac7

Graphics

A gist of the Python code used for data summaries and graphics is available at:

https://gist.github.com/mamacneil/f55d48278a8ba4073983b7e2b4ab0e06

Additional References

31. Wenban-Smith, N. & Carter, M. Chagos: A history: exploration, exploitation, expulsion. Chagos Conservation Trust, London (2016).

32. Sheppard, C.R.C, *et al.* Reefs and islands of the Chagos Archipelago, Indian Ocean: why it is the world's largest no-take marine protected area. *Aquat Conserv Mar Freshw Ecosyst* **22,** 232-261 (2012).

33. Graham, N. A. J., McClanahan, T. R., MacNeil, M. A., Wilson, S. K., Cinner, J. E., Huchery, C. & Holmes, T. H. Human disruption of coral reef trophic structure. *Curr Biol* **27,** 231-236 (2017).

34. Readman, J.W. *et al.* in *Coral Reefs of the United Kingdom Overseas Territorie*s (ed. Sheppard, C. R. C.) Contaminants, pollution and potential anthropogenic impacts in Chagos/BIOT. 283-298 (Springer, Netherlands, 2013).

35. Bibby, C.J., Burgess, N.B. & Hill, D.A. Bird Census Techniques. Academic Press Ltd, London (1992).

36. McGowan, A., Broderick, A.C. & Godley, B.J. Seabird populations of the Chagos Archipelago: an evaluation of Important Bird Area sites. *Oryx* **42,** 424-429 (2008).

37. del Hoyo, J., Elliott, A., Sargatal, J., Christie, D. A. & de Juana, E. (Eds.). Handbook of the Birds of the World Alive. Lynx Edicions, Barcelona. http://www.hbw.com (2017).

38. Krzywinski, M. & Altman, N. Points of significance: visualizing samples with box plots. *Nature Methods* **11,** 119-120 (2014).

39. Jennings S, Collingridge K 2015 Predicting consumer biomass, size-structure, production, catch potential, responses to fishing and associated uncertainties in the world's marine ecosystems. PLoS One 10, e0133794

40. http://www.mercator-ocean.fr/ Mercator Ocean require the following statement accompanies use of their GCM data. The data are © Mercator Ocean. Product and interpretations obtained from Mercator Ocean products. Mercator Ocean cannot be held responsible for the results nor for the use to which they are put. All rights reserved.
41. Aumont O, Bopp L 2006 Globalizing results from ocean in situ iron fertilization studies, Global Biogeochemical Cycles, 20, GB2017.
42. Mendez, L. *et al.* Geographical variation in the foraging behaviour of the pantropical red-footed booby. *Mar Ecol Prog Ser* **568,** 217-230 (2017).
43. Schmidtko S, Johnson GC, Lyman JM 2013 MIMOC: A global monthly isopycnal upper-ocean climatology with mixed layers. Journal of Geophysical Research 118: 1658-1672
44. BODC 2008 The GEBCO Digital Atlas published by the British Oceanographic Data Centre on behalf of IOC and IHO.
45. Ashmole, N. P. Body size, prey size, and ecological segregation in five sympatric tropical terns (Aves: Laridae). System Zool 17, 292-304 (1968).
46. Harrison, C. S., Hida, T. S. & Seki, M. P. Hawaiian seabird feeding ecology. Wildlife Monogr 85, 3-71 (1983).
47. Wiebe PH, Boyd SH, Cox JL (1975) Relationships between zooplankton displacement volume, wet weight, dry weight and carbon. Fishery Bulletin 73, 777–786
48. Jennings, S. & Cogan, S.M. (2015) Nitrogen and carbon stable isotope variation in northeast Atlantic fishes and squids. Ecology, 96, 2568.
49. Martiny, A.C., Vrugt, J.A. & Lomas, M.W. (2014) Concentrations and ratios of particulate organic carbon, nitrogen, and phosphorus in the global ocean. Scientific Data, 1, 140048.
50. Martiny, A. C., J. A. Vrugt, F. W. Primeau, and M. W. Lomas (2013), Regional variation in the particulate organic carbon to nitrogen ratio in the surface ocean, Global Biogeochem. Cycles, 27, 723–731.
51. Crossland, C.J., Hatcher, B.G. & Smith, S.V. (1991) Role of coral reefs in global ocean production. Coral Reefs, 10, 55-64.
52. Hatcher, B G (1990) Coral reef primary productivity: a hierarchy of pattern and process. Trends in Ecology and Evolution 5: 149-155.
53. Salvatier, J., Wiecki, T. V. & Fonnesbeck, C. Probabilistic programming in Python using PyMC3. *PeerJ Computer Sci* **2,** e55 (2016).
54. Gelman, A., Carlin, J. B., Stern, H. S., Dunson, D. B., Vehtari, A., & Rubin, D. B. Bayesian data analysis (Vol. 2). CRC Press, Boca Raton (2014).
55. Campana, S. E. Otolith science entering the 21st century. *Mar Freshwater Res* **56,** 485-495 (2005).
56. Pardo, S. A., Cooper, A. B., & Dulvy, N. K. Avoiding fishy growth curves. *Methods Ecol Evol* **4,** 353-360 (2013).
57. Wilson, S.K., Graham, N.A.J. & Polunin, N.V.C. Appraisal of visual assessments of habitat complexity and benthic composition on coral reefs. *Mar Biol* **151,** 1069-1076 (2007).

58. Froese, R. & Pauly, D. FishBase. http://www.fishbase.org (2015).
59. Letourneur, Y. Length-weight relationships of some marine fish species in Reunion Island, Indian Ocean. *Naga ICLARM Quarterly* **21,** 36-39 (1998).
60. Wilson, S.K. *et al.* Exploitation and habitat degradation as agents of change within coral reef fish communities. *Global Change Biol* **14,** 2796-2809 (2008).
61. Ong, L. & Holland, K. N. Bioerosion of coral reefs by two Hawaiian parrotfishes: species, size differences and fishery implications. *Mar Biol* **157,** 1313-1323 (2010).
62. McDuie, F., Weeks, S. J., Miller, M. G. R. & Congdon, B. C. Breeding tropical shearwaters use distant foraging sites when self-provisioning. *Mar Ornithol* **43,** 123–129 (2015).
63. Calabrese, L. Foraging ecology and breeding biology of wedge-tailed shearwater (Puffinus pacificus) and tropical shearwater (Puffinus bailloni) on Aride Island Nature Reserve, Seychelles : tools for conservation. Doctoral dissertation, Université Pierre et Marie Curie-Paris VI (2015).
64. Pennycuick, C. J., Schaffner, F. C., Fuller, M. R., Obrecht III, H. H. & Sternberg, L. Foraging flights of the white-tailed tropicbird (Phaethon lepturus): radiotracking and doubly-labelled water. *Colon Waterbirds* **13,** 96-102 (1990).
65. Jaquemet, S., Le Corre, M., Marsac, F., Potier, M. & Weimerskirch, H. Foraging habitats of the seabird community of Europa Island (Mozambique Channel). *Mar Biol* **147,** 573–582 (2005).
66. Gilardi, J. D. Sex-specific foraging distributions of brown boobies in the eastern tropical Pacific. *Colon Waterbirds* **15,** 148–151 (1992).
67. Weimerskirch, H., Le Corre, M., Jaquemet, S. & Marsac, F. Foraging strategy of a tropical seabird, the red-footed booby, in a dynamic marine environment. *Mar Ecol Prog Ser* **288,** 251–261 (2005).
68. Surman, C. A. & Wooller, R. D. Comparative foraging ecology of five sympatric terns at a sub-tropical island in the eastern Indian Ocean. *J Zool* **259,** 219–230 (2003).
69. Bourne, W. R. P. & Simmons, K. E. L. The distribution and breeding success of seabirds on and around Ascension in the tropical Atlantic Ocean. *Atlantic Seabirds* **3,** 187-202 (2001).
70. Dunlop, J. N. Foraging range, marine habitat and diet of bridled terns breeding in Western Australia. *Corella* **21,** 77–82 (1997).
71. Hulsman, K. & Smith, G. Biology and growth of the black-naped tern (*Sterna sumatrana*): A hypothesis to explain the relative growth rates of inshore, offshore and pelagic feeders. *Emu* **88,** 234–242 (1988).

Data availability statement

Data used for figures 1-4 in this paper are available through the GitHub links in the Methods.

Code availability

Code used for figures 1-4 in this paper are available through the GitHub links in the Methods.

Extended Data Figure 1 | Primary production and potential prey biomass and production in areas accessible to seabirds foraging around the Chagos Islands. a) recorded foraging ranges for seabird species that feed on smaller prey (light tone, 0.1 to 9 g individual wet weight) or larger prey (dark tone, 1 to 50 g individual wet weight; broken lines indicate greater ranges are expected for two species and foraging area calculations assume the foraging range is the radius of the foraging area), b) primary production in the foraging area, c) modelled biomass, and d) production of fauna in the foraging area (median and 90% uncertainty intervals based on 10,000 simulations to assess the effects of parameter uncertainty[39] on biomass or production estimates). Biomass and production were estimated for fauna in the prey size ranges consumed by each bird species, and expressed as wet or nitrogen (N) weight.